Structure of 22,12-Polyurethane in Chain-Folded Lamellar Crystals

Robin L. McKiernan,† Pawel Sikorski,‡ Edward D. T. Atkins,*,‡ Samuel P. Gido,† and Jacques Penelle†

Department of Polymer Science and Engineering, University of Massachusetts, Amherst, Massachusetts, 01003-4530 and Physics Department, University of Bristol, Tyndall Avenue, Bristol, BS8 1TL, U.K

Received May 14, 2002; Revised Manuscript Received July 16, 2002

ABSTRACT: Aliphatic 22,12-polyurethane has been crystallized directly from the melt and isothermally at 105 °C from *N*,*N*-dimethylformamide to give chain-folded lamellae of thickness ≈ 14 nm. The crystals have been investigated using X-ray diffraction, electron microscopy (imaging and diffraction), and computer modeling. The diffraction data was used to establish that the chains crystallize in a single-chain, triclinic unit cell, and the structure bears a strong resemblance to chain-folded lamellar crystals of even−even nylons. The results show that, even for a molecule with relatively long alkane segments, the hydrogen bonds exercise a controlling influence on the crystallization process and crystalline structure. Two models were investigated: one based on an analogy with nylon 6 6 and the other derived using molecular dynamics; they both turned out to be closely related. The model generated using molecular dynamics predicted localized rotations at the termini of the ester−amide coupled units. The resolution of the experimental data was not sufficient to clearly delineate between the two models, but the separate calculations do provide an estimate of the tolerances that can be accepted.

Introduction

We have recently compared the crystallization behavior, characterization and properties of a series of linear, aliphatic *m*,*n*-polyurethanes, based on the generalized repetitive chemical repeat unit: [O−$(CH_2)_m$−O−**CONH**−$(CH_2)_n$−**NHCO**], where m = 12, 22, or 32 and n = 4, 6, 8, or 12.[1−4] These syncephlic[5] chain molecules were synthesized by step polyaddition of the appropriate aliphatic diol and diisocyanate. In general, it was found that this polyurethane family crystallized from both the melt and solution in the form of thin (≈10−18 nm) lamellae and the estimated chain length was an order of magnitude greater than the measured lamellar thicknesses, and therefore, chain-folding is expected in these lamellar crystals.[3] This preceding investigation[3] established that, although respectably long alkane segment lengths were incorporated, with consequential reduction in the frequency of amide units along the backbone, the interamide hydrogen bonding remained the dominant feature in the crystallization process and the room-temperature crystalline structure. In short, the behavior was more akin to the even−even nylons[6−11] (e.g., nylon 6 6[6,7]) than polyethylene[12,13] or the corresponding aliphatic polyesters.[14]

In this paper we focus on, and describe in more detail, the structure of the lamellar crystals obtained from the 22,12-polyurethane molecule, since it gave the best combined data set from X-ray diffraction, transmission electron microscopy, and selected area electron diffraction and was representative of the overall structural features and generalized crystallization behavior of this family of even−even aliphatic polyurethanes.[3]

Experimental and Modeling Section

Materials. The synthesis and characterization of the 22,12-polyurethane −[O−$(CH_2)_{22}$−O−C(O)−NH−$(CH_2)_{12}$−NH−C(O)]$_x$− have already been reported in detail.[1]

* Corresponding author: E-mail: e.atkins@bristol.ac.uk. Fax: +44 1179-255624.
† University of Massachusetts, Amherst.
‡ University of Bristol.

Crystal Preparation. Crystals were prepared by melting the polymer at 200 °C and allowing the sample to cool to room temperature at a rate of 10 °C min^{-1}. Solution-grown crystals were prepared by dissolving the 22,12-polyurethane in *N*,*N*-dimethylformamide (DMF) at 120 °C (temperature maintained in an oil bath) to make a 0.01% (w/v) solution. The temperature was rapidly cooled to room temperature and then slowly reheated to the temperature (115 °C) where the polymer dissolved. The temperature was gradually lowered over a period of 1 h to 105 °C and isothermally crystallized for 20 h before being allowed to cool to room temperature. Oriented crystal mats suitable for X-ray diffraction were prepared by allowing the crystal suspension to drain through a 0.22 μm filter and excess DMF was washed off. The resulting flakes consist of crystalline lamellae sedimented on top of each other but with random orientation about the lamellar normal.

X-ray Diffraction. X-ray diffraction patterns, in the medium to wide-angle range, were obtained at room temperature using nickel-filtered Cu Kα radiation of wavelength 0.1542 nm from a sealed tube X-ray generator operating at 40 kV and 30 mA. A point-collimated beam was used and the X-ray diffraction patterns were recorded using a flat image plate in an evacuated Statton camera. Calcite (d_b = 0.3035 nm) was dusted onto selected samples for calibration purposes. X-ray scattering patterns, in the small-angle range, were obtained at room temperature using nickel-filtered Cu Kα radiation of wavelength 0.1542 nm from a Rigaku rotating anode operating at 40 kV and 200 mA. A point-collimated 300 μm diameter beam was used, and the X-ray diffraction patterns were recorded using a two-dimensional area detector.

Transmission Electron Microscopy. Carbon-coated transmission electron microscopy (TEM) grids were dipped into the crystal suspension, and the solvent was allowed to evaporate in a vacuum oven at room temperature. Some samples were shadowed with Pt/Pd to enhance the contrast of the TEM images, while other samples were shadowed with gold to calibrate the electron diffraction patterns. The TEM images and electron diffraction patterns were recorded at room temperature using a JEOL 100 CX microscope operating at 100 kV.

Model Building. The software package Cerius2, version 3.8 (MSI) was used in structural modeling and diffraction simulations. The software packages InsightII and Discover3 (MSI), employing the CVFF force field, were used in the molecular dynamics simulations. Periodic boundary conditions,

10.1021/ma020739o CCC: $22.00
Published on Web 09/18/2002

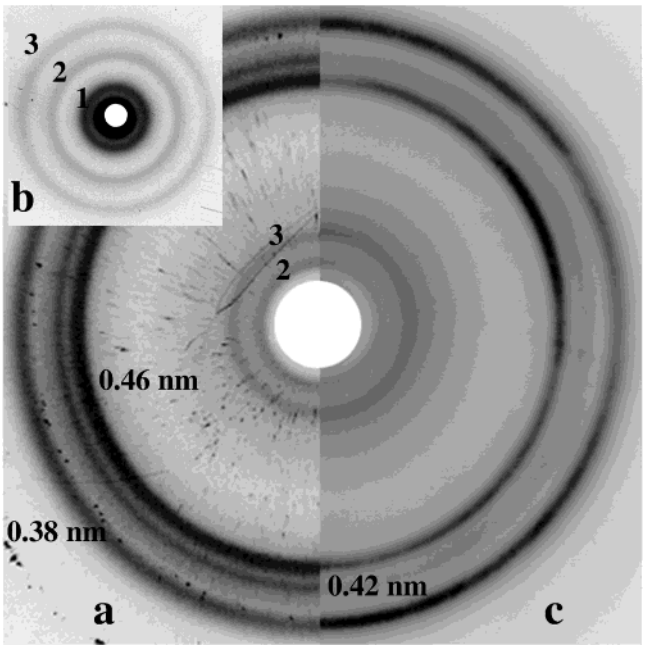

Figure 1. Wide and medium-angle X-ray diffraction patterns from chain-folded crystalline lamellae of 22,12-polyurethane. (a) Wide-angle pattern obtained from unoriented melt-crystallized sample. The sharp spots and streaks are from the calibrant. The second and third orders of the 36.0 nm periodicity are present. (b) Medium-angle pattern showing fundamental (1) and orders (2 and 3) of the 36.0 nm spacing associated with the chain axis structural periodicity. (c) Wide-angle pattern obtained from aggregates of the material isothermally crystallized in DMF. Partial orientation is evident by the circumferential fluctuations in intensity. The second and third orders of the 36.0 nm periodicity are again evident.

with bonds across the boundaries in the chain direction, were used in these dynamic simulations. The Ewald summation method was used in the calculation of nonbonded interactions. The simulations were performed at 298 K under constant pressure and temperature assembly conditions (NPT), and consisted of 50000 MD steps in 1 fs intervals.

Results and Discussion

X-ray Diffraction. The X-ray diffraction pattern, in the medium to wide-angle range, for crystals of 22,12-polyurethane crystallized from the melt is shown in Figure 1a. There is no preferred orientation and the Bragg diffraction signals appear as rings. The wide-angle has two intense rings at *d* spacings of 0.46 and 0.38 nm, respectively. We shall show later that these diffraction signals represent the predominant interchain spacings orthogonal to the chain axis of the crystal lattice, i.e., *hk*0 diffraction signals. In addition, a weaker diffraction ring occurs at a *d* spacing of 0.42 nm. In even−even nylons, a diffraction spacing with this value is often identified with some pseudohexagonal crystalline phase being present.[9] We shall discuss the origin of this diffraction ring in more detail later when specific structural models for 22,12-polyurethane are considered. Two other medium-angle diffraction rings appear closer to the center of the pattern at *d* spacings of 1.20 and 1.80 nm, respectively. These two diffraction rings are in fact the second and third orders, respectively, of a fundamental structural repeat of 3.60 nm. This is confirmed by the diffraction pattern (Figure 1b insert) recorded at larger specimen to detector distance, where the fundamental and its orders are clearly seen. It will be shown later that this 3.60 nm spacing represents a projection, owing to chain tilt, of the structural repeat along the chain, or *c* axis, direction. A similar X-ray diffraction pattern, with essentially the same *d* spacings, is obtained from solution-crystallized aggregates of 22,12-polyurethane as shown in the comparative Figure 1c. Here one can notice fluctuations in intensity around the circumferences of the diffraction rings suggesting partial orientation of the crystalline entities. Using small-angle X-ray scattering (SAXS) a single diffraction peak was discovered at a *d* spacing of 13.9 nm, as illustrated in the low-angle diffraction trace shown in Figure 2. We interpret this diffraction signal as the lamellar stacking periodicity (LSP) of the chain-folded lamellar-like crystals.

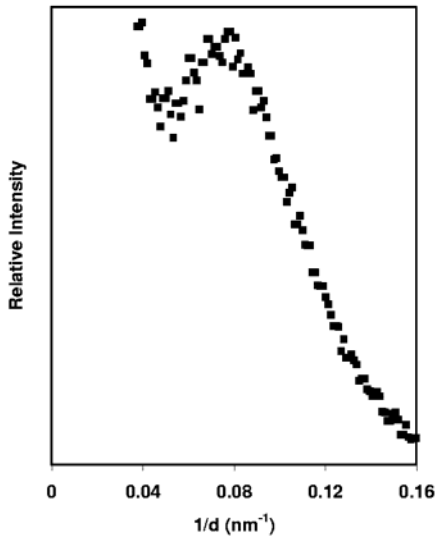

Figure 2. SAXS trace from 22,12-polyurethane crystals showing the lamellar stacking periodicity (LSP) at 13.9 nm.

The 22,12-polyurethane isothermally crystallized at 105 °C from the melt and the solution-crystallized samples gave essentially the same diffraction spacings (within the limits of experimental error), including the LSP value. Sedimented mats of the solution-grown crystals gave X-ray diffraction patterns exhibiting a degree of orientation and texture. When the incident X-ray beam is directed parallel to the mat surface, with the mat normal vertical, an oriented diffraction pattern is obtained, as shown in Figure 3. The three successive orders of the 3.60 nm periodicity mentioned previously appear as meridional arcs and the interchain (*hk*0) wide-angle arcs appear at various angular rotations with respect to the meridional direction. These features bear similarities to the diffraction patterns obtained from sedimented mats composed of stacked lamellae of nylon 6 6[7] and other even−even nylons[8−11] and suggests that the chains are tilted with respect to the lamellar surface normal. Indeed, the periodicity of 3.60 nm offers us a direct measure of the chain tilt since it represents the interplanar d_{001} spacing. If we assume, at this stage, that the chain conformation is a planar zigzag[15] the *c* axis identity period of the 22,12-polyurethane molecule is calculated to be 5.03 nm; thus, the angle of chain tilt with respect to the lamellar surface normal is $\cos^{-1}(3.60/5.03) = 44.3°$. The X-ray diffraction pattern obtained of the sedimented mat with the incident beam normal to the mat shows a series of diffraction rings. Thus, the sedimented mat consists of a stack of lamellae, all with their surface normals coincident and parallel to the *c** axis; i.e., the X-ray pattern shown in Figure 3 represents

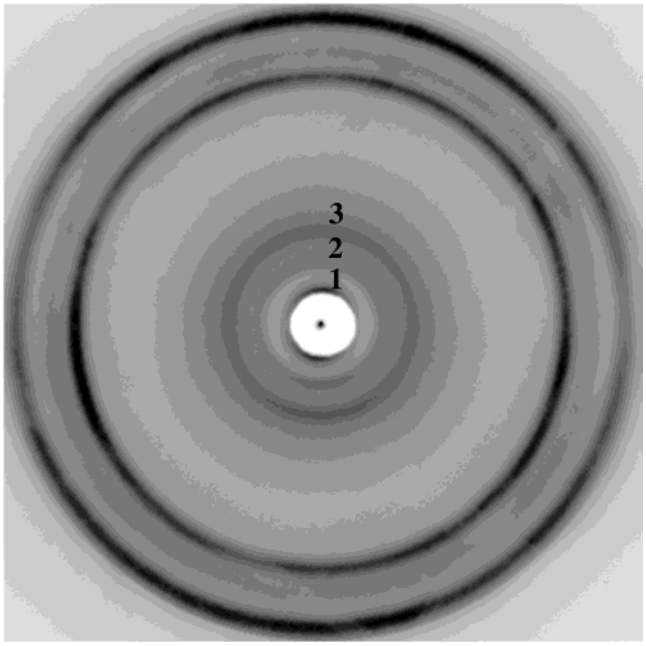

Figure 3. X-ray diffraction pattern obtained from a sedimented mat of 22,12-polyurethane isothermally crystallized from DMF at 105 °C. The incident beam is parallel to the mat surface and the mat normal is vertical. The three orders of the 36.0 nm periodicity along the meridian are labeled.

Table 1. Comparison of Observed and Calculated *d* Spacings, Estimated Observed Relative Intensities, and Real and Reciprocal Unit Cell Parameters

22,12-polyurethane		model A				model B			
d_{obs} (nm)	obsd intens	d_{cal} (nm)	h	k	l	d_{cal} (nm)	h	k	l
0.453 ± 0.002	vs	0.450	1	0	0	0.457	1	1	2
						0.447	1	1	$\bar{1}$
0.422 ± 0.002	m	0.428	1	0	$\bar{4}$	0.418	1	0	$\bar{2}$
						0.423	1	0	$\bar{3}$
0.376 ± 0.002	s	0.379	0	1	0	0.378	0	1	0
3.60 ± 0.02	vs	3.6	0	0	1	3.63	0	0	1
1.80 ± 0.01	s	1.8	0	0	2	1.81	0	0	2
1.20 ± 0.005	m	1.2	0	0	3	1.21	0	0	3

LSP = 13.9 ± 0.2

	model A	model B	nylon 6 6
a, nm	0.51	0.49	0.49
b, nm	0.58	0.59	0.54
c, nm	5.03	4.85	1.72
α, deg	46	54	48.5
β, deg	77	87	77
γ, deg	63	59	63.5
a^*, nm^{-1}	0.220	0.253	0.229
b^*, nm^{-1}	0.270	0.264	0.271
c^*, nm^{-1}	0.028	0.027	0.078
α*, deg	133	13	130
β^*, deg	82	69	84
γ^*, deg	115	127	114
$a \wedge a^*$, deg	28	37	27
$b \wedge b^*$, deg	49	50	47
$c \wedge c^*$, deg	44	41	42

a rotation photograph with the c^* axis directed along the meridian (vertical bisector). A summary of the diffraction spacings, together with estimates of relative intensities and indexing, is given in Table 1.

Electron Microscopy. (a) Real Space Imaging. Figure 4 shows the lamellar crystals obtained from a 40 nm microtomed slice of a ruthenium oxide-stained, melt-crystallized sample. The (white) lamellae have equal and constant thickness. Since we envision these lamellae to be chain-folded, care needs to be exercised in recording the actual thickness, since it is not certain how deep the ruthinum oxide stain penetrates the lamellar surface layer; measurement suggests a minimum thickness of ≈13 nm. This result is wholly consistent with the 13.9 nm LSP value measured in the SAXS experiments. Figure 5a shows an image of the isothermally crystallized, solution-grown crystals of 22,-12-polyurethane; extended aggregates of overlaying lathlike lamellae. The thickness of individual lamella in the enlarged area (Figure 5b), using metal shadowing, is estimated to be ≈14 nm.

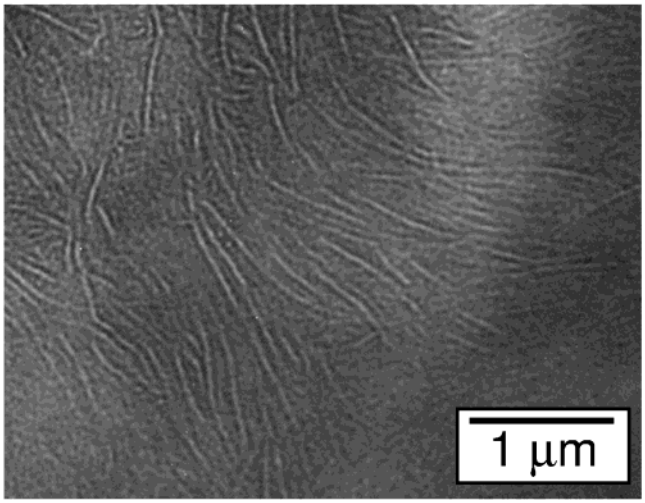

Figure 4. Transmission electron micrograph of microtomed sections of melt-crystallized 22,12-polyurethane stained with ruthenium oxide. The lamellar crystals are white.

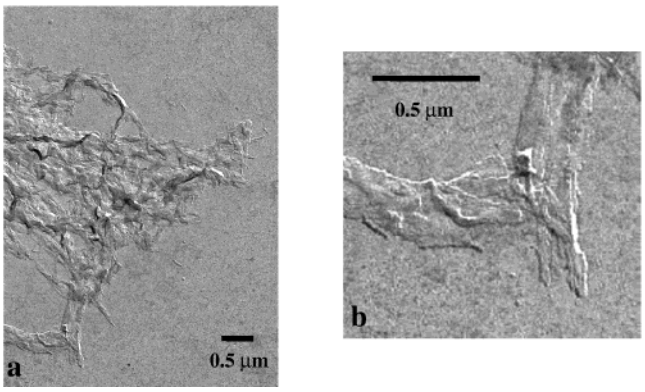

Figure 5. Transmission electron micrographs of 22,12-polyurethane isothermally crystallized from DMF at 105 °C and shadowed with Pt/Pd: (a) general view; (b) enlarged selected area where the estimated lamellar thickness is 14 nm. (Shadowing angle 40° gave an average measured shadow of 16.7 nm on the original micrograph for the single layer crystal edges orthogonal to the source of evaporated metal.)

(a) Electron Diffraction. We know from the analysis of the X-ray diffraction data shown in Figure 3 that the c^* axis in an individual lamella is parallel to its surface normal, and therefore, the c axis, or chain axis, will be at an approximate angle of 44.3° and in a precisely defined direction with respect to the crystallographic axes.[16] Therefore, to obtain the [001] zone electron diffraction from an individual lamella (Figure 5b), the sample has to be tilted by a large angle in a specific direction, and such a selected area electron diffraction procedure is technically demanding; the

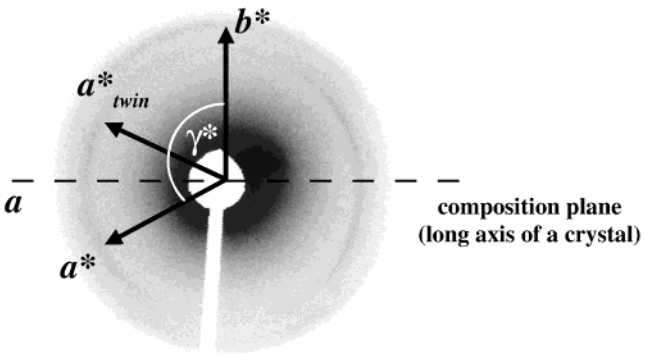

Figure 6. Selected area electron diffraction taken with the incident beam parallel to the overall chain direction. This is the [001] zone axis in model A and would represent the a^*b^* reciprocal plane and giving γ^* directly. It represents the [$\bar{2}$01] zone for model B, and the indices of the diffraction signals are given in Table 1; in this case the labeling is not correct.

electron diffraction pattern only lasts for seconds owing to beam damage. However, we did manage to achieve it experimentally as illustrated in Figure 6. This [001] zone electron diffraction pattern is useful since it records the a^*b^* reciprocal net and allows us to measure γ^* directly; a value of 115 ± 2° was found. Figure 6 also shows that twining occurs, typical of chain-folded crystals of nylons,[8−11] and that the composition plane is (010) and is parallel to the long axis of the crystalline lamella. Indeed, the combination of electron diffraction, X-ray diffraction, and electron microscopy imaging data closely resembles that of the single-chain triclinic structures of chain-folded lamellar crystals of even−even nylons.[8−11]

Unit Cell Parameters and Structural Modeling

We realize a priori, from the quality of the oriented crystal lamellae obtained, that the diffraction data is not sufficient to support a detailed structure determination, along the lines, for example, of nylon crystalline 6 6 fibers[6] or oligoamide crystalline lamellae.[17,18] However, there are some structural features that are desirable to examine in more detail. We have chosen to explore two types of crystal structure models, based on two different modeling strategies, in an attempt to obtain a better understanding of the molecular interactions involved in the crystallization of 22,12-polyurethane and to ensure that stereochemically feasible structures for 22,12-polyurathane can be generated to match the basic and limited diffraction data.

Strategy 1. The combined X-ray and electron diffraction of 22,12-polyurethane closely resembles that of the nylon 6 6-like single-chain, triclinic structure and therefore we have a basic structural scaffolding to aid our analysis. On the basis of the lamellar structures of the even−even nylons,[8−11] we can obtain, from the selected electron diffraction pattern (Figure 6), values for γ^*, d_{100}, and d_{010}. From the X-ray diffraction data (Figure 3), we can determine the angle $c \wedge c^*$ (assuming an all-trans chain conformation). If the 22,12-polyurethane chains hydrogen bond together in a cooperative manner, like the p-sheets of nylon 6 6,[10,7−11,6] then β = 77° and the value of c = 5.03 nm. On the basis of these assumptions, the triclinic unit cell, a = 0.51 nm, b = 0.58 nm, c = 5.03, α = 46°, β = 77°, and γ = 63°, can be derived. The calculated density is 1.04 g cm^{-3}. These values are compared with the nylon 6 6 in Table 1 and are within a 7% maximum difference, apart of course for the distinctly different c value. The structure (model A) of 22,12-polyurethane based on this unit cell is shown in Figure 7. The chains associate into chain-folded fully saturated hydrogen-bonded nylon-like p-sheets (Figure 7a), with a folding periodicity provided by the experimentally recorded LSP value. Figure 7b shows a view parallel to the chain (c) axis of the hydrogen-bonded sheets stacking via van der Waals forces and progressively shearing in the ac planes in the a direction. The sheets also have substantial progressive ac plane shear in the c direction (Figure 7c). Thus, this 22,12-polyuethane triclinic structure is conceptually similar to nylon 6 6 chain-folded lamellar crystals.[7]

Figure 8a shows the X-ray diffraction pattern of this structure, generated using the Cerius2 computer program and incorporating the appropriate correction factors, and may be compared directly with the experimentally recorded X-ray diffraction pattern shown in Figure 3. As can be seen, the basic features are the same, including interestingly enough the generation of a diffraction signal at 0.43 nm[19] diffraction arc in Figure 8a. We shall discuss the occurrence of this 0.43 nm diffraction arc in detail later; suffice to say at this stage that it is not a $hk0$ diffraction arc (10 $\bar{4}$, see Table 1). The unit cell parameters and comparison of measured and calculated d spacings are given in Table 1.

We could, of course, be satisfied with this analysis of the data, bearing in mind the limited nature of the diffraction data. However, we have tended to develop and construct this model on the basis of a conceptual comparison with even−even nylons. At this stage, we judged it prudent to consider examining the 22,12-polyurethane structure using a different approach, in an attempt to ascertain possible variations and limitations on the overall theme. After all, in the model shown in Figure 7, the implantation of the ester units adjacent to the amide units in the backbone appear to have had little effect on the crystalline structure.

Strategy 2. In this case, molecular dynamic (MD) simulations were used to find an optimal chain conformation, the preferred mode of chain packing and unit cell. The starting model consisted of 22,12-polyurethane chains, in the all-trans conformation, sited at the corners of a tetragonal lattice with sides $a = b$ = 0.7 nm and c = 5.03 nm, i.e., the interchain (a, b) distances were in excess of what we know to be the final values in the fully crystalline state. To minimize the effect of the periodic boundary conditions imposed, calculations were performed in a super cell that consisted of 36 polymer chains; with each chain composed of two chemical repeats in length, i.e., a super-cell of 6 × 6 × 2 unit cells. The starting setting angle of the chain was chosen to be distinctly different to that found in nylon 6 6[6] and other[8−11] even−even nylon crystal structures. The system was subjected to MD simulation procedures and in the process the system density and chain conformation was allowed to change in order to minimize the overall potential energy of the system. No constrains were placed on the 22,12-polyurethane chain conformation or unit cell parameters. Thus, this final structure (model B) is a consequence of the intra- and interchain interactions and their interplay, the crystalline structural features being determined by factors such as hydrogen-bonding, influence (mutual and otherwise) of the ester and amide units on the chain conformation and van der Waals interactions between the relatively long alkane segments.

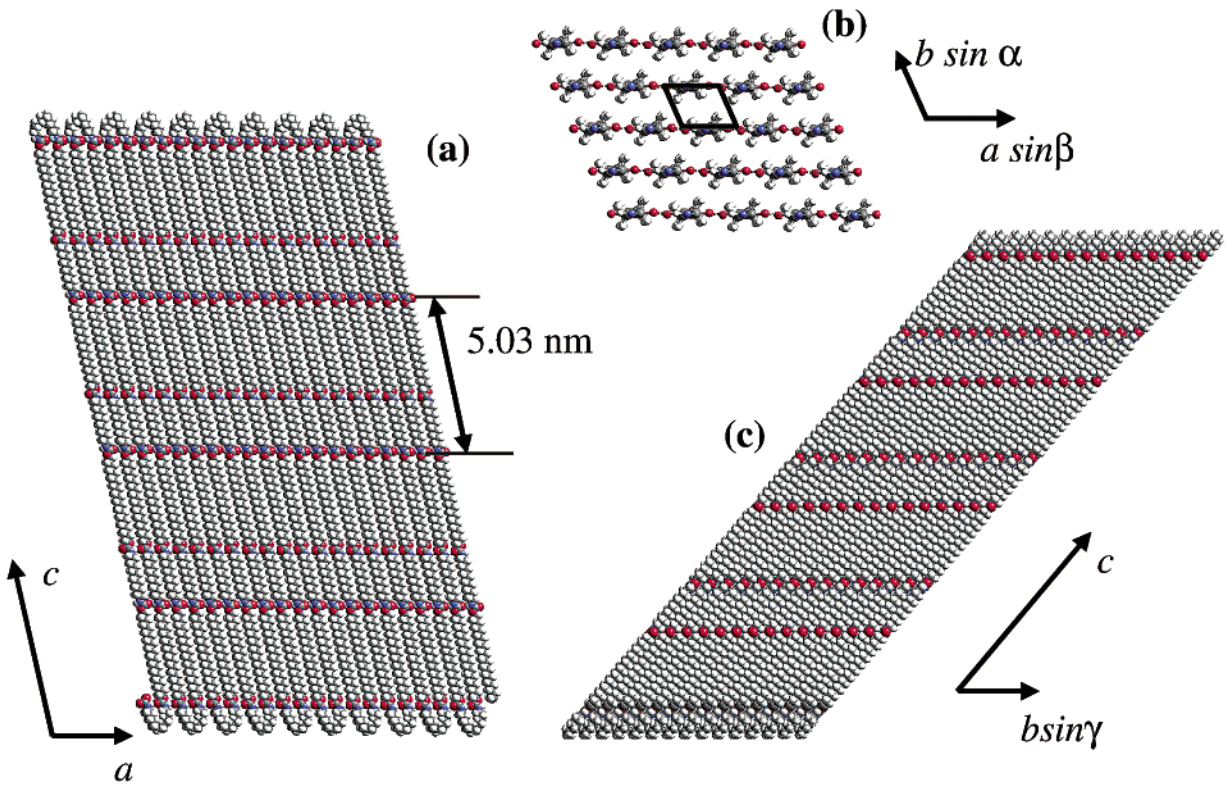

Figure 7. Structural model A based on nylon 6 6[6,7] and other even−even nylon triclinic single-chain crystal structures. (a) View of p-sheets (orthogonal to *ac* plane) of 22,12-polyurethane hydrogen-bonded sheets in space-filling mode and folding, via the alkane segments, in a manner to form a chain-folded structure commensurate with the measured LSP value. Key: red, oxygen; blue, nitrogen; black, carbon; white, hydrogen. (b) Ball and stick view parallel to chain, or *c* axis, of straight-stem portion of crystal. The hydrogen bonds are shown as dashes in the horizontal direction; the box represents the projection of the unit cell; the color code is as in part a. (c) View, in space-filling mode, orthogonal to *a* axis (hydrogen-bond direction) of the progressively sheared hydrogen-bonded sheets. Color code is as in part a.

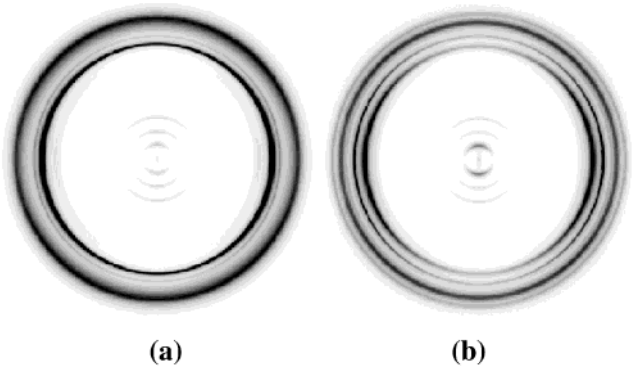

Figure 8. Computer generated simulated X-ray diffraction patterns from sedimented mats of 22,12-polyurethane lamellar crystals. (a) The pattern derived from model A (Figure 7) based on the even−even nylon p-sheet/progressive sheet shear triclinic structures with an all-trans chain conformation. This predicts an additional 0.43 nm diffraction signal in the equatorial region. (b) The pattern derived by applying modeling strategy 2. The additional additional diffraction signal is at 0.42 nm.

The resulting structure is shown in Figure 9, and the X-ray diffraction pattern generated using the Cerius2 program is shown in Figure 8b. The unit cell is triclinic with the following parameters: $a = 0.49$ nm, $b = 0.59$ nm, $c = 4.85$, $\alpha = 54°$, $\beta = 87°$, and $\gamma = 59°$. The *d* spacings and other geometric information are given in Table 1. The calculated density is 1.08 g cm^{-3}. Comparison of the computer-generated X-ray diffraction pattern (Figure 8b) and the experimental pattern (Figure 3) is good. The structure also generates the 0.42 nm diffraction signal. The salient features of this crystal structure are summarized as follows. The chains form hydrogen-bonded sheets (*ac* plane) but with noticeable self-correcting or recuperative kinks in the localized region of the coupled ester amide backbone implantations as illustrated in Figure 9a. These chain kinks emanate from 10° torsional rotations, from all-trans, about the terminal bonds of the −OC(O)N− units (see Figure 9).[20] The alkane segments remain in the all-trans conformation. The sheets stack with progressive shear in the *a* and *c* directions parallel to the *ac* planes similar to the previous model (Figure 7). Since the slip in the *c* direction is small (0.35 nm; 0.40 nm in model A), the alkane segments of juxtapositioned sheets remain parallel; i.e., there is no "crossing" of chain directions between contiguous ones that would lead to poorer intersheet packing. This is illustrated in Figure 9a, where we show that a second sheet is lying on top of the underlying first sheet.

Examination of the real and reciprocal unit cell parameters of model B in Table 1 reveal that there are two noticeable differences compared with model A. The first is that, naturally, the value of *c* is reduced by 3.6% as a consequence of the recuperative intra-sheet kinking (see Figure 9a). More significantly, the value of γ^* is increased to 127° (10.4%) and at first sight appears to contradict the measured value of 115° (see Figure 6 and Table 1). However, it needs to be appreciated that, for model B, the selected area electron diffraction pattern shown in Figure 6 is now the [$\bar{2}$01] zone and therefore does not measure γ^* directly. In this case the labeling in Figure 6 would need to be modified, since the angle,

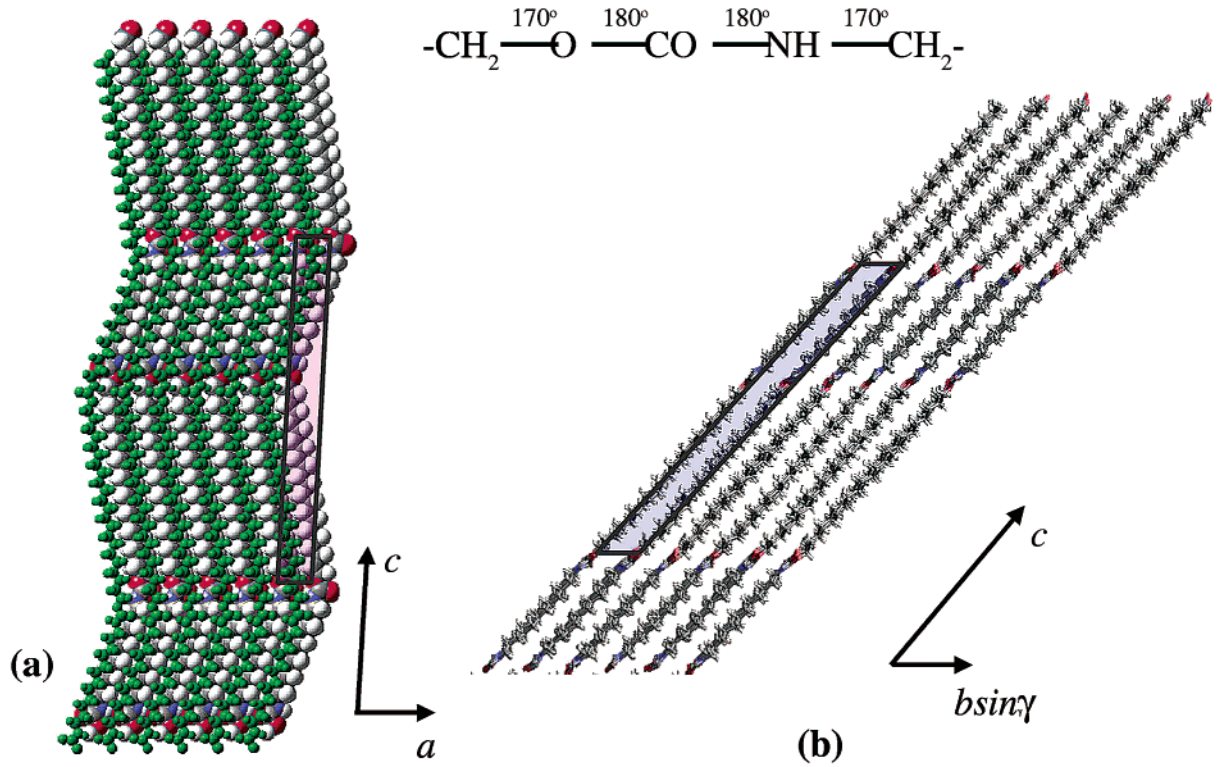

Figure 9. Structural model B based on the modeling strategy 2. The projections of the unit cell are represented by the boxes. (a) A pair of overlaid sheets viewed orthogonal to the *ac* plane. The underlying sheet is in space-filling mode and color code as for Figure 7. The overlying (ball and stick) sheet is in green. (b) View parallel to the *a* axis.

denoted by γ^*, is now a projection of γ^*, and the diffraction signals are not *hk*0. The actual indices are given in Table 1. The model B data in Table 1 illustrate this point; the strong arcs in the X-ray and electron diffraction are not all *hk*0 diffraction signals; e.g., the strong 0.45 nm arc is the combined 112 and 111 diffraction signals. It needs to be remembered that the *c* value is large (≈5 nm), and therefore, reciprocal planes with $l = 1$ or 2 contribute. Indeed in model B the [$\bar{2}$01] zone axis contains the strong interchain diffraction signals. The three strong diffraction signals found in the calculated X-ray pattern (Figure 8b; Table 1) match the experimental spacings 0.45, 0.42, and 0.38 nm favorably.

General Discussion and Conclusions

The two structures, models A and B, shown in Figures 7 and 9, respectively, are meant to indicate the tolerances involved in structural analyses based on the limited diffraction data available from the 22,12-polyurethane lamellar crystals. We do not intend to seriously delineate between them. However, we will point out their respective merits and weaknesses. We will also discuss the occurrence of the equatorial diffraction signal in the region of 0.42 nm.

The basic structure for the 22,12-polyurethane lamellar crystals is of chain-folded hydrogen-bonded sheets in which the dipoles are aligned and there is some intrasheet shearing (Figures 7a and 9a). The sheets stack with progressive shear (Figures 7b and 9b) to give a single-chain, triclinic structure. Thus, the general direction of the chains (*c* axis), is substantially tilted (44° for model A; 41° for model B) to the crystalline lamellar normals. This type of architecture is similar to that reported for the even−even nylons.[8−11]

Table 1 provides a comparison of the 22,12-polyurethane models with that of nylon 6 6. However, the 22,12-polyurethane *c* repeat is about three times that of the nylon 6 6, and therefore, the 00*l* reciprocal planes are more closely spaced. In addition, the limited crystal thickness (≈14 nm) lengthens the reciprocal lattice points in the *c** direction and, together with partial disorientation, enables strong diffraction signals with *h* and *k* of 0 or 1 and *l* small, but not zero, to diffract. Thus, for example in model A (Figures 7 and 8a and Table 1), a diffraction signal appears at 0.43 nm 10 $\bar{4}$ in addition to the 100 (0.45 nm) and 010 (0.38 nm) pair, characteristic of nylon 6 6. A similar situation occurs with model B Figures 9 and 8b and Table 1). In this case the matching of the 0.42 nm diffraction signal (combined 10 $\bar{2}$ and 10 $\bar{3}$) is even better. The 0.45 nm diffraction signal also has nonzero values for *l*. Indeed, Figure 8b (model B) matches the experimental pattern (Figure 3) better than Figure 8a (model A). The azimuthal rotation, about the equatorial line, for the 0.45 nm arcs are ±7° (±8° for model A), and for the 0.38 nm diffraction signal, they are ±41° (±43° for model A). Model B also incorporates kinks in the otherwise all-trans backbone. In polyesters, similar bond rotations have been reported as cited in a recent review.[14]

Analysis of the structural data, even though limited, firmly supports the contention[3] that the 22,12-polyurethane molecule behaves in a manner closely resembling that of the even−even nylons, rather than, e.g., polyethylene. This implies that the hydrogen bonds maintain a controlling influence on both the crystallization and crystalline structure. The analysis underlying model B suggests that the ester units or extended alkyl segments would like to impart localized rotations, resulting in recuperative kinks in the backbone, but

without destroying the intrasheet hydrogen bond network.

The 0.42 nm diffraction signal has also been observed in nylons and is usually interpreted in terms of another pseudohexagonal phase.[19] In light of this structural investigation of 22,12-polyurethane, the diffraction data from some of the higher nylons perhaps should be examined.

Finally, we wish to briefly mention the folding periodicity. The 22,12-polyurethane was crystallized by cooling from the melt (T_m = 200 °C) and isothermally at 105 °C in *N*,*N*-dimethylformamide, with the same folding periodicity (LSP 13.9 nm, Table 1). There is no fundamental reason why they should be the same, nor does it have to be wholly coincidence. The syncephlic 22,12-polyurethane molecule has to fold with a discrete number of structural units to form a regular lamella, as discussed previously, for example in nylons.[7,21] Thus, the lamellar thickness has to change by quite large and discrete steps, owing to the relatively large value of the *c* repeat. Thus, it is not too surprising that the same lamellar thickness is found using both methods of crystallization in this particular case since the conditions are not too different.

Acknowledgment. This work is supported by NSF Material Research Science and Engineering Center (MRSEC) (NSF Grant No. DMR-9809365) at UMASS, and the Engineering and Physical Sciences Research Council (EPSRC) at Bristol University. We are grateful to EPSRC for a postdoctoral fellowship to P.S. E.D.T.A. was a Visiting Professor at the Department of Polymer Science and Engineering, University of Massachusetts, during part of this research collaboration. The use of MRSEC central experimental facilities and the W. M. Keck Polymer Morphology Laboratory at the University of Massachusetts is acknowledged. We thank the Bristol Moecular Recognition Center for access to molecular software.

References and Notes

(1) McKiernan, R. L.; Gido, S. P.; Penelle, J. *Polymer* **2002**, *43*, 3007.
(2) Heintz, A. M.; McKiernan, R. L.; Gido, S. P.; Penelle, J.; Hsu, S. L. *Macromolecules* **2002**, *35*, 3117.
(3) McKiernan, R. L.; Heintz, A. M.; Hsu, S. L.; Atkins, E. D. T.; Penelle, J.; Gido, S. P. *Macromolecules* **2002**, *35*, 6970.
(4) McKiernan, R. L.; Cardoen, G.; Boutevin, B.; Améduri, B.; Gido, S. P.; Penelle, J. Submitted to *Macromol. Chem. Phys.* In this particular contribution, hetroatom segments were inserted into the polyurethane backbone.
(5) The term *syncephlic* signifies head-to-head, tail-to-tail polymerization; thus, the resulting polymer has no polarity with respect to chain direction. In this sense, these molecules relate to, for example, the even−even nylon family.
(6) For fibers: Bunn, C. W.; Garner, E. V. *Proc. R. Soc. London, Part A* **1947**, *189*, 39.
(7) For chain-folded lamellar crystals of nylon 6 6: Atkins, E. D. T.; Keller, A.; Sadler, D. M. *J. Polym. Sci. A* **1972**, *2*, 863. For examples of other even−even nylons see refs 8−11.
(8) Atkins, E. D. T.; Hill, M. J.; Hong, S. K.; Keller, A.; Organ, S. *Macromolecules* **1992**, *25*, 917.
(9) Jones, N. A.; Atkins, E. D. T.; Hill, M. J. *J. Polym. Sci., Polym. Phys.* **2000**, *38*, 1209.
(10) Jones, N. A.; Atkins, E. D. T.; Hill, M. J.; Cooper, S. J.; Franco, L. *Macromolecules* **1997**, *30*, 3569.
(11) Atkins, E. D. T.; Hill, M. J.; Jones, N. A.; Cooper, S. J. *J. Polym. Sci., Polym. Phys.* **1998**, *36*, 2401.
(12) Geil, P. H. *Polymer Single Crystals*; Interscience: New York, 1963.
(13) Keller, A. *Prog. Phys.* **1968**, *31*, 41.
(14) Le Fevere de ten Hove, C.; Jones, A.; Penelle, J. Submitted to *Macromolecules*.
(15) This value can be modified later as part of the refinement process.
(16) The value of 44.3° for the tilt angle is dependent on the value chosen for *c*, and therefore might alter slightly in the refinement process. The direction of tilt, with respect to the unit cell axes, will be determined by the structural model proposed.
(17) Atkins, E. D. T.; Hill, M. J.; Jones, N. A.; Sikorski, P. *J. Mater. Sci.* **2000**, *35*, 5179.
(18) Sikorski, P.; Atkins, E. D. T. *Macromolecules* **2001**, *34*, 4788.
(19) A 0.42 nm diffraction signal in nylons is often associated with a pseudohexagonal phase being present, e.g. ref 9.
(20) Calculation of the torsional energy profiles of the CH_2−NH and O−CH_2 bonds showed that the global energy minimum is for the all-trans conformation (180, 180°) and that the energy penalty for distortion of the all-trans conformation by less than 20° is small (∼5 kJ/mol). In the case of model B, the increase in the potential due to perturbed all-trans conformation of the CH_2−NH and O−CH_2 bonds (170, 170°) is compensated for by an increase in the van der Waals interaction energy due to better chain packing. In general, the shortening of the chain may not be a consequence of the conformation preferred by an isolated chain but instead may be influenced by packing of chains, especially of the long alkane segments.
(21) Magill, J. H.; Girolamo, M.; Keller, A. *Polymer* **1981**, *22*, 43.

MA020739O